Molecular Crystals and Liquid Crystals

Publication details, including instructions for authors and subscription information:
http://www.tandfonline.com/loi/gmcl20

Dyeing Crystals to Dyeing Tissues: Congo Red in Anisotropic Media

Miki Kurimoto [a], Beat Müller [a], Werner Kaminsky [a], Bart Kahr [a] & Lee-Way Jin [b]

[a] Department of Chemistry, and Department of Pathology, University of Washington, Seattle, WA, 98195-1700

[b] Department of Pathology, University of Washington, Seattle, WA, 98195-1700

Version of record first published: 18 Oct 2010

To cite this article: Miki Kurimoto, Beat Müller, Werner Kaminsky, Bart Kahr & Lee-Way Jin (2002): Dyeing Crystals to Dyeing Tissues: Congo Red in Anisotropic Media, Molecular Crystals and Liquid Crystals, 389:1, 1-9

To link to this article: http://dx.doi.org/10.1080/10587250216139

Mol. Cryst. Liq. Cryst., Vol. 389, pp. 1–9

1058-725X/02 $12.00 + .00
DOI: 10.1080/10587250290191767

Taylor & Francis
Taylor & Francis Group

DYEING CRYSTALS TO DYEING TISSUES: CONGO RED IN ANISOTROPIC MEDIA

Miki Kurimoto, Beat Müller, Werner Kaminsky, and Bart Kahr[*]
Department of Chemistry, and Department of Pathology, University of Washington, Seattle, WA 98195-1700

Lee-Way Jin
Department of Pathology, University of Washington, Seattle, WA 98195-1700

In the past, we have studied the process of dyeing crystals through measurements of linear optical anisotropies (e.g., linear dichroism and linear birefringence). Techniques for analyzing the optical properties of dyed crystals are readily translated to stained crystalline tissues, countless examples of which have been described by chemical histologists. Moreover, questions pertaining to mechanisms of non-covalent association are comparable whether the structured host is a single crystal or crystalline tissue. Here, the azo dye, Congo red, in two types of anisotropic media, sucrose single crystals and fibrous, proteinaceous amyloid plaques, is described. Optical micrographs of amyloid from the brains of deceased Alzheimer's Disease patients made with a newly developed imaging system reveal previously unrecognized features. As formation of ordered amyloid plaques from their relatively small peptides may well be considered a pathological biocrystallization process, a clear understanding of the deposition mechanism may lead to strategies for crystallization inhibition.

Keywords: dyeing crystals; birefringence imaging; amyloid; Congo red; Alzheimer's Disease

INTRODUCTION

In the recent past we have studied the process of dyeing crystals whereby a great range of substances was shown to have the remarkable ability to

LWJ thanks the National Institute of Aging (2P50 AG 05136). BK thanks the National Science Foundation (CHE-0092617). BK and WK thank the Petroleum Research Fund of the American Chemical Society (35706-AC6) for support of this research.

[*]Corresponding author

orient and overgrow chromophores present in solution [1]. Crystal dyeing is, and has been, an idiosyncratic enterprise that can be traced to the 1854 studies of Sénarmont who prepared artificially pleochroic crystals of $Sr(NO_3)_2 \cdot 4H_2O$ when grown in the presence of the extract of logwood, a tree rich in the dye precursor, hematoxylin [2]. In contrast to the process of dyeing crystals, the dyeing of structures found in tissues, many of which are highly anisotropic, is an enormous field of inquiry, chemical histology [3], that has played a central role in the development of pathology; in fact, hematoxylin is probably the most commonly used stain in histology. Since both the processes of dyeing crystals and dyeing tissues are governed by the specificity of non-covalent interactions that can lead to ordered arrays of visible chromophores, we began to consider whether our experience with the former might inform the latter.

Ambronn was the first and to the best of our knowledge the only scientist who considered both subjects, crystal and tissue dyeing. Best remembered for his observation of linear dichroism from dye-stained cell membranes [4], he also observed the linear dichroism from the azo dye,

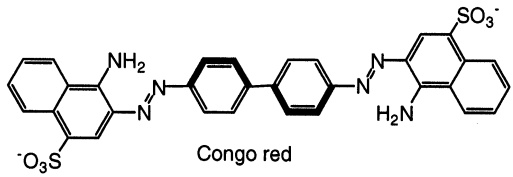

Congo red

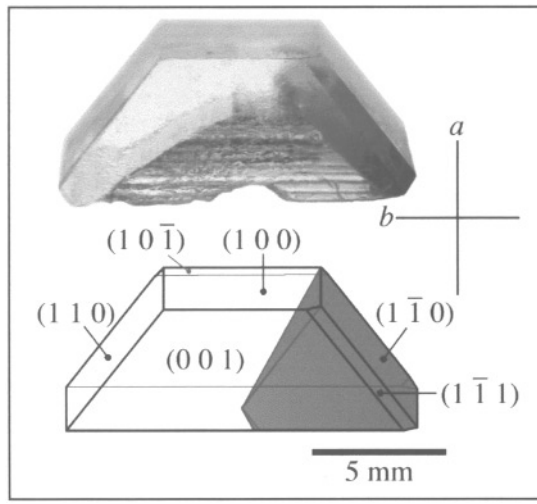

FIGURE 1 Top: Sucrose crystal grown in the presence of Congo red. The view is parallel to the polar *b* axis. Bottom: Idealized representation. (See Color Plate I)

Congo red (CR), aligned within a sucrose crystal [5]. While no adequate crystallographic description of his dyed sucrose crystals was given, we reproduced the phenomenon as shown in Figure 1, and have observed that the $\{1\ \bar{1}\ 0\}$ faces [6] are those that recognize the dye. The adsorption is polarized in the *bc* plane.

In our laboratories, we have used CR to dye growing K_2SO_4 crystals. CR is just one of many dyes that have the ability to stain particular K_2SO_4 growth sectors [7]. Shown in Figure 2 is a micrograph of a polished section of a K_2SO_4 crystal, grown in the presence of CR. A schematic representation of the crystal habit is also shown. The absorption is strongly polarized along [100] when viewed in this projection.

Congo red is most widely used for studying amyloid, insoluble proteinaceous deposits [8] that are associated with many disorders, including Alzheimer's Disease. Amyloid is 'Congophilic'; it absorbs CR and when stained displays a characteristic linear dichroism and linear birefringence that are used in the *post mortem* diagnosis of Alzheimer's Disease. The anisotropy arises because amyloid plaques, while not single crystals, are aggregates of highly anisotropic fibrils made from peptides (39–43 amino acids) arranged as twisted, laminated β-sheets [9].

Are there common features or salient differences to be elucidated in the processes of dyeing salt crystals and neural tissues with CR? Here, we explore the possibility that extending our purview to tissues will give us

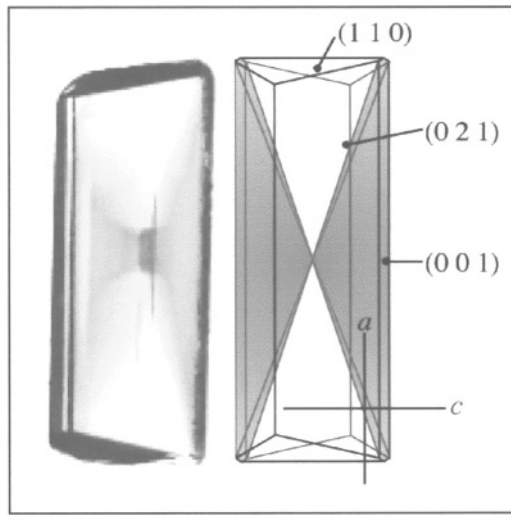

FIGURE 2 Left: Polished section (4 mm high, ~100 μ thick) of crystal of K_2SO_4 grown in the presence of Congo red. The dye recognizes the {0 0 1} growth sectors. Right: Idealized representation. (See Color Plate II)

greater understanding of the staining of anisotropic media with CR generally, and perhaps provide insights into the formation of pathological structures.

CONGOPHILIC AMYLOID

Congo red, a spectacularly successful textile dye, was synthesized by Böttinger at Baeyer in 1883 [10]. The first scientific applications followed immediately [11]. In 1922 its specific association with amyloid was identified [12]. A standard procedure for staining amyloid with CR was established by Puchtler *et al.* in 1962 [13] who surmised that the dye was attached via unspecified hydrogen bonds and "ionic linkages". Lillie [14] invoked hydrogen bonding as the major mechanism of association as did Glenner *et al.*, [15] Davies and Mera [16], and Turnell and Finch [17], but Glenner [15] assigned equal importance to hydrophobic interactions, the principal non-covalent interaction according to Pigorsch *et al.* while Davies and Mera [16] invoked van der Waals forces, the principle non-covalent interaction according to Horobin [19]. Turnell and Finch, leaving no stone unturned, cited the importance of hydrophobic and van der Waals interactions in addition to H-bonding. Ionics forces were specified by Klunk *et al.* [20] as well as Puchtler [21] who later favored "non-ionic" interactions, similarly preferred by Katenkamp and Stiller [22]. More recent experiments were aimed as specifying more precisely the CR point(s) of attachment. Kirschner [23] and coworkers identified histidine residues as most "Congophilic". Cavillon *et al.* [24] preferred arginine while Li *et al.* [25] liked lysines (as well as hydrophobic interactions). It is safe to conclude that the process of amyloid staining by CR is not fully understood.

Irrespective of the staining mechanism, simple inspection with a polarizing microscope can nevertheless provide information about the orientation of the dyes within amyloid plaques. However, there does not seem to be a consensus as to whether the transition dipole moments of the CR molecules are parallel [22,26] or perpendicular [25,27] to the fiber axes. Clearly, new methods for the optical analysis of CR stained amyloid would be desirable in order to identify the dyeing mechanism. First and foremost, however, is an understanding of the electronic structure of Congo red.

ELECTRONIC STRUCTURE OF CONGO RED

While there is little doubt, from what we know of comparable molecules, that the visible electric dipole transition moments are nearly parallel with the long axis of the molecule we nevertheless confirmed our expectation

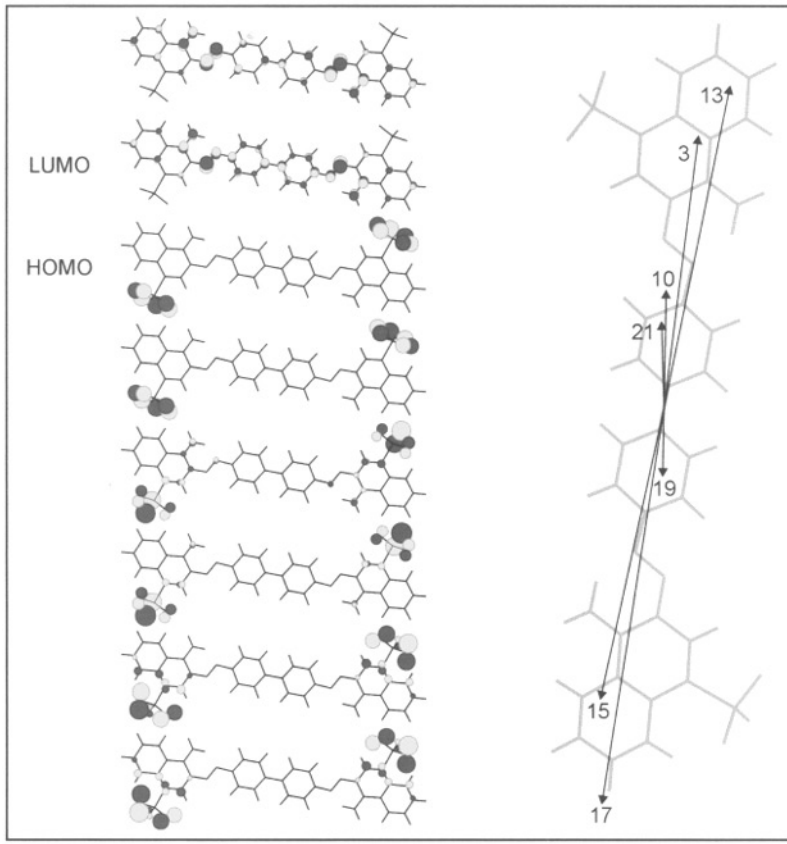

FIGURE 3 Molecular orbitals (HOMO-5 to LUMO+1) and electric dipole transition moments of the 7 strongest excitations (out of 30) calculated by td-B3L YP/3-21G for *trans*-**CR**. (See Color Plate III)

computationally, building on the work previously carried out by Roterman and workers [28]. We performed geometry optimizations on the double anion of the two main conformers *cis*- and *trans*-CR on B3LYP/3-21G and HF/3-21G level, respectively. Both conformers have a C_2 axis perpendicular to the biaryl C–C bond. The *trans* conformer was calculated to be 1.2 kcal/mol more stable than the *cis* conformer (corrected for zero point vibrational energy). Frequency calculations established that the geometries represented real minima. The biaryl dihedral angles were 39.5° for *cis*- and 35.4° for *trans*-CR at B3LYP/3-21G level and increased to 51.6° and 45.6° respectively at HF/3-21G level. The lowest vibrational frequencies are the

torsional moieties associated with the biaryl linkage - their values were calculated to be between 6.5 and 8.5 cm^{-1} for both methods and conformers.

To calculate the electric dipole transition moment we performed time dependent td-B3LYP calculations of the first 30 transitions using the 3-21G basis set. The results for the *cis* and *trans* conformers were essentially the same. The two lowest energy transitions involving the HOMO and HOMO-1 have negligible oscillator strengths as do transition with components along the C_2 axes. The strong transitions are all nearly parallel with the long molecular axis (Fig. 3). They are invariably charge transfer excitations from the sulfonate groups (HOMO-2 to HOMO-13) into the aminodiazoaryl π-system (LUMO and LUMO+1).

LINEAR BIREFRINGENCE AND LINEAR DICHROISM IMAGING

When an anisotropic sample such as CR stained amyloid is viewed in transmission through crossed polarizers, the commonly observed interference colors actually arise from the convolution of several effect: absorption, linear birefringence (Δn), linear dichroism (ΔA), and extinction (θ, describing orientation of the refractive index tensor).

Only just now can we separate these effects from one another using the recently invented imaging system of Kaminsky, Glazer and coworkers of Oxford University [29,30]. In this method, light (I_0) is passed through a polarizer which is rotated by an angle α with a stepper motor. The intensity of the light passing through the sample and a circular analyzer is measured with a CCD camera as a function of α. By modulating the intensity as a function of α, $I/I_0(\alpha)$ for each pixel is subject to a Fourier separation of the disparate contributions to the intensity including the transmittance, retardation ($\delta = 2\pi L\Delta n/\lambda$, the extent to which the eigenmodes propagating through the sample are out of phase), and θ. Without the analyzer the system images ΔA where θ' indicates the eigenmodes for absorption. The essential equations appear below [31,32].

$$\frac{I}{I_0} = \frac{1}{2}\left[1 + \sin^2(\alpha - \theta)\sin\left(2\pi L\frac{\Delta n}{\lambda}\right)\right] \tag{1}$$

$$\frac{I}{I_0} = \cosh\left(\frac{2\pi\Delta AL}{\lambda}\right) + \sinh\left(\frac{2\pi\Delta AL}{\lambda}\right)\cos(2\pi - 2\theta') \tag{2}$$

Such an imaging system has transformed our ability to study heterogeneous dyed crystals by instantaneously revealing variations in ΔA as a function of growth history or growth sector specificity, or variations in Δn associated with impurity induced strain [1].

OPTICAL IMAGING OF CONGO RED STAINED AMYLOID

What can we learn about amyloid using this new microscope described in the previous section? As well stated by Steensma: "At the dawn of the 21st century . . . the diagnostic test of choice [for amyloidosis] has not changed in decades . . . Congo red is still the 'king of dyes'[33]." Therefore, it may well be of value to bring the latest methods for the optical analysis of heterogeneous substances to bear on the characterization of CR stained amyloid. We applied the Oxford technique to amyloid from the brains of deceased Alzheimer's Disease patients. The images that we have thus far produced

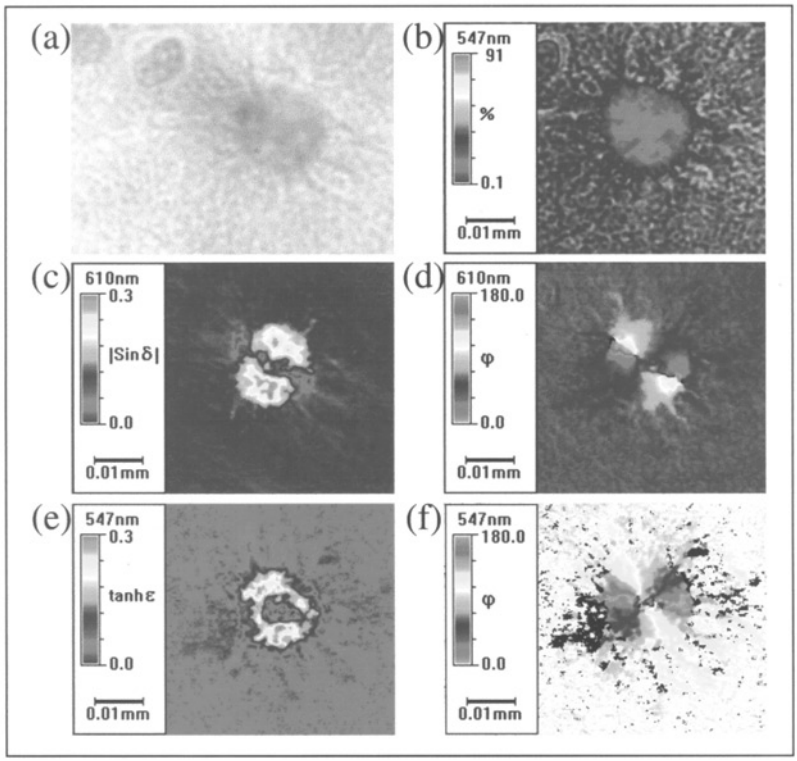

FIGURE 4 Linear birefringence and linear dichroism imaging of cerebral Alzheimer's amyloid plaque stained with CR (×600). (a) CR stained plaque in white light, (b) % transmission solely attenuated by absorption, (c) function of the retardation, $|sin\,\delta|$, where $\delta = 2\pi\Delta nL/\lambda$, (d) extinction angles, θ (deg), showing radial order, (e) tanh(ε) which is a quantity associated with the linear dichroism where ε is the extinction coefficient, and (f) θ (deg) the orientation of the electric transition dipole moments. (See Color Plate IV)

are far more detailed than those produced using conventional microscopies (Fig. 4). Compare the ordinary image of CR stained amyloid absorption (Fig. 4a: this is what the pathologist sees *post mortem*) with those made by the new technique. While the round plaque seems to be homogeneous in transmission (Fig. 4b) with radially order (Fig. 4d), there is a disordered hole in the center as evidenced by the fact that $|\sin\delta| = 0$ in Figure 4c. The hole is mimicked in the map related to linear dichroism (Fig. 4e) which is given as the hyperbolic tangent of the extinction coefficient, ϵ. Figure 4f shows the direction of maximum absorbance in degrees from horizontal axis. The slow direction in Figure 4d corresponds with the direction of maximum absorbance because there is a significant resonance enhancement of the refractive index from the absorption of CR. Dispersive effects were measured off resonance at 610 nm whereas dissipative effects were measured in the absorption band at 547 nm.

Such structures resemble spherulites, aggregates built from concentric rings of small crystallites that many crystallographers often discard as products of a failed crystallizations. Have growth conditions changed such that the outer portion has begun to crystallize around a disordered core? Is the disordered plaque crystallizing from the outside in like a geode? Surely, such questions regarding the mechanisms of crystal aggregate growth are of importance for the design of strategies to inhibit the deposition of pathogenic amyloid plaques. Despite the fact that our inquiry is in its infancy, it is clear that optical micrographs of dyes associated with anisotropic structures reveal aspects of amyloid formation that are not discernable in electron or atomic force micrographs aimed at the identification of individual fibrils [34].

REFERENCES

[1] Kahr, B. & Gurney, R. W. (2001). *Chem. Rev., 101*, 893.
[2] Sénarmont, H. (1854). *Ann. Phys. Chem., 167*, 491; Sénarmont, H. (1854). *Ann. Chim. Phys., 3*, 319.
[3] Clark, G. (1983). *History of Staining*, Williams and Wilkens, Baltimore.
[4] Ambronn, H. (1888). *Ber. Dtsch. Bot. Ges., 6*, 85.
[5] Ambronn, H. (1889). *Ber. Dtsch. Bot. Ges., 7*, 103.
[6] Döhl, B. & Follner, H. (1992). *Cryst. Res. Technol., 27*, 3; Sgualding, G., Aquilano, D., Vaccari, G., Mantovani, G., & Salamone, A. (1998). *J. Cryst. Growth, 192*, 290.
[7] Bastin, L. D. & Kahr, B. (2000). *Tetrahedron, 56*, 6633.
[8] Sipe, J. D. (1994). *Crit. Rev. Clin. Lab. Sci. 31*, 325.
[9] Lynn, D. G. & Meredith, S. C. (2000). *J. Struct. Biol., 130*, 153.
[10] Böttinger, P. (1884). *Deutsches Reichs Patent*, 28753, August 20.
[11] Griesbach, H. (1886). *Z. Wissen. Mikroskopie Mikroskopische Technik, 3*, 358.
[12] Benhold, H. (1992). *Münchener Mediz. Wochen. 69*, 1537.
[13] Puchtler, H. Sweat, F., & Levine, M. (1962). *J. Histochem. Cytochem. 10*, 355.

[14] Lillie, R. D. (1977), in ***H. J. Conn's biological stains***, 9th ed.; The Williams & Wilkins Co.: Baltimore, pp 147–148.
[15] Glenner, G. G., Eanes, E. D., Bladen, H. A., Linke, R. P., & Termine, J. D. (1974). ***J. Histochem. Cytochem. 22***, 1141.
[16] Davies, J. D. & Mera, S. L. (1983). ***Bristol Med. Chir. J. 98***, 90.
[17] Turnell, W. G. & Finch, J. T. (1992). ***J. Mol. Biol. 227***, 1205.
[18] Pigorsch, E., Elhaddaoui, A. & Turrell, S. (1994). ***Spectromchim. Acta.*** 50A, 2145.
[19] Horobin, R. W. (1980). ***J. Microsc. 119***, 345.
[20] Klunk, W. E., Pettegrew, J. W., & Abraham, D. J. (1989). ***J. Histochem. Cytochem. 37***, 1273.
[21] Puchtler, H., Waldrop, F. S. & Meloan, S. N. (1985). ***Appl. Pathol. 3***, 5.
[22] Katenkamp, D. & Stiller, D. (1972). ***Histochemie, 29***, 37.
[23] Krischner, D. A., Inouye, H., Duffy, L. K., Sinclair, A., Lind, M. & Selkoe, D. J. (1987). ***Proc. Natl. Acad. Sci. USA, 84***, 6953.
[24] Cavillion, F., Elhaddaoui, A., Alix, A. J. P., Turrell, S. & Dauchez, M. (1997). ***J. Mol. Struct. 408/409***, 185.
[25] Li, L., Darden, T. A., Bartolotti, L., Kominos, D. & Pedersen, L. G. (1999). ***Biophys. J. 76***, 2871.
[26] Wolman, M. & Bubis, J. J. (1965). ***Histochemie, 4***, 351; Missmahl, H. P. (1996). ***Introd. Quant. Cytochem.*** 1, 539; Taylor, D. L., Allen, R. D., & Benditt, E. P. (1974). ***J. Histochem. Cytochem.*** 22, 1105; Glenner, G. G. & Page, D. L. (1976). ***Int. Rev. Exp. Pathol.*** 15, 1.
[27] Cooper, J. H. (1974). ***Lab, Invest.*** 31, 232; Elhaddaoui, A., Pigorsch, E., Delacourte, A. & Turrell, S. (1995). ***J. Mol. Struct.*** 347, 363; Carter, D. B. & Chou, K. -C. (1998). ***Neurobiol. Aging***, 19, 37.
[28] Skowronek, M., Roterman, I., Konieczny, L., Stopa, B., Rybarska, J., Piekarska, B., Górecki, A. & Król, M. (2000). ***Comput. Chem. 24***, 429.
[29] Glazer, A. M., Lewis, J. G. & Kaminsky, W. (1996). ***Proc. R. Soc. London, A Mat. 452***, 2751.
[30] Geday, M. A., Kaminsky, W., Lewis, J. G. & Glazer, A. M. (2000). ***J. Microscopy, 198***, 1.
[31] Born, M. & Wolf, E. (1980). ***Principles of Optics, 6***th ***ed.***, Cambridge University Press, Cambridge.
[32] A comparable device, but based on ferroelastic modulators has been demonstrated recently (R. Oldenbourg & G. Mei, ***J. Microscopy, 180***, 140 (1995)) that has been beautifully applied to the imaging of filamentous actin (Katoh, K., Hammer, K., Smith, P. J. S. & Oldenbourg, R. (1999). ***Mol. Biol. Cell. 10***, 197; Katoh, K., Hammer, K., Smith, P. J. S. & Oldenbourg, R. (1999). ***Proc. Natl. Acad. Sci. USA, 96***, 7928; Danuser, G. & Oldenbourg, R. (2000). ***Biophys. J. 79***, 191; Oldenbourg, R., Katoh, K. & Danuser, G. (2000). ***Biophys. J.*** 78, 1176.) and microtubules (Oldenbourg, R., Salmon, E. D., Tran, P. T. (1998). ***Biophys. J.*** 74, 645).
[33] Steensma, D. P. (2001). ***Arch. Pathol. Lab. Med. 125***, 250.
[34] McLaurin, J., Yang, D.-S., Yip, C. M. & Fraser, P. E. (2000). ***J. Struct. Biol. 130***, 259.